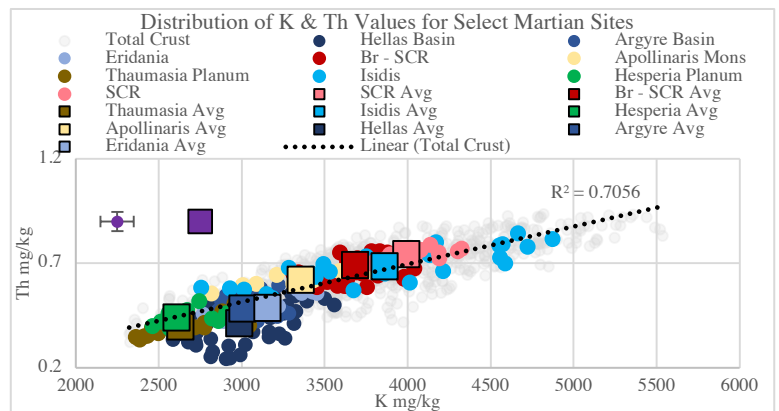


**EVIDENCE FOR SUPERVOLCANIC RESURFACING IN ARABIA TERRA, MARS.** Augustus Bates<sup>1</sup>, Suniti Karunatillake<sup>1</sup>, Sander Goossens<sup>2</sup>, Lujun Ohja<sup>3</sup>, Juan Lorenzo<sup>1</sup> <sup>1</sup>Louisiana State University, Geology and Geophysics ([abate15@lsu.edu](mailto:abate15@lsu.edu)), <sup>2</sup>University of Maryland, Baltimore, <sup>3</sup>Rutgers University

**Introduction:** The Arabia Terra region is one of the oldest Martian landscapes, and shows evidence of paterae eruptions similar to terrestrial supervolcanoes [1]. These potentially represent a new class of volcanism on Mars [1]. The structures could be remnants of early, explosive-style volcanism on Mars, in contrast to the effusive volcanism that dominated the landscape later in the planet’s history [2]. As such, they hold great potential to link Noachian-aged explosive volcanism to several large-scale geologic events that resurfaced much of Arabia Terra. However, it is unknown if the paterae-bearing region is geochemically consistent with volcanism. Geochemical similarities between Arabia Terra and contemporaneous, Noachian-aged Martian volcanic and sedimentary provinces could help identify if Arabia Terra was once subject to super-volcanic eruptions. In addition, if this region did host paterae volcanism, the style of eruption can be examined from a geophysical perspective. Further analysis of the Arabia Terra region can lead to a greater understanding of the planet’s geologic evolution and provide insight into the early surface conditions on Mars.

In this study, gamma ray spectrometer (GRS) regional geochemistry from the two delineated areas within Arabia Terra, the supervolcanic context region (SCR) and the broad-SCR [3], are compared to the contemporaneous Martian volcanic and sedimentary analogs (fig. 1). Comparative analysis and interpretation of regional geochemical trends serves to form a cohesive narrative for the emplacement of the unique chemistry observed within Northwest Arabia Terra. We also present geophysical data derived from gravitational modeling based on observed topography. These results help to bound the overall load density of SCR and its elastic thickness, which can function as a proxy for thermal flux.

**Methodology:** The GRS suite [4] of chemical data, with a focus on concentrations of K and Th, allows us to examine the possibility of igneous activity (K, Th) as well as possible aqueous alteration (K, Th) within a regional Martian context [6,7]. The map by Tanaka et. al [5] was used to identify contemporaneous volcanic sites and major sedimentary provinces elsewhere on Mars. The volcanic sites consist of Thaumasia Planum, Hesperia Planum and Apollinaris Mons and the sedimentary provinces are Isidis, Argyre, Hellas and portions of Eridania Planum to the East of Hellas. The basins were chosen based on areal extent, to ensure reasonable chemical coverage and contemporaneous age. Eridania serves as a proxy for heavily eroded, fine-grained material which was sourced from various provenances [5], making it a useful chemical proxy for retaining eolian fines. Using the coordinates of the outlined areas, chemical data were compiled for all the sites and plotted in bivariate space (K, Th) to examine regional trends among all regions.



**Figure 2:** Average K & Th values for selected Martian geologic features in mg/kg. A linear average trendline is fitted to the data, and errors are approximated for the averages in the upper left (square) and for the underlying data (circle).

For the geophysical analysis, we compute localized correlations and admittance between gravity and topography using a cap with a radius of 15° (centered on -5°E, 25°N) and a bandwidth of  $L_{win}=30$  for the localization window [6]. We use a degree and order 150 expansion of Mars’ gravity field [8]. We find correlations > 0.8 (corresponding to a signal-to-noise ratio better than 1.78 [6]) for spherical harmonics degrees > 77 for our chosen localization. We thus use the degree range 77-120 to fit theoretical admittance models that depend on the following parameters: crustal density, load density, crustal thickness, elastic thickness, load depth, and load

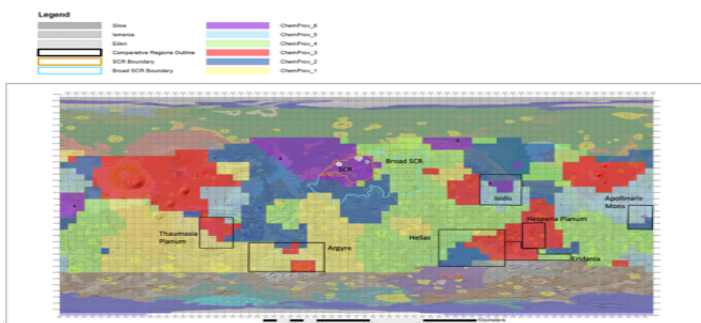


**Figure 1:** Geologic map of Mars [5] with the geochemical provinces from Taylor et al., 2010 overlain. The SCR and broad SCR are shown along with the proposed paterae from [1]. The black boxes outline our GRS delineations of our comparative regions.

ratio. We apply a straightforward grid search to find the best-fit admittance models in this degree range, by computing the theoretical admittance for each parameter combination, and applying the same downward continuation (to the average radius of the area of interest, 3390 km) and localization as we applied to the measured admittance.

**Results:** Among our reference regions, we observe the highest average abundance of K and Th (Fig. 1) within SCR, with the second highest average in Isidis. The broad SCR is third in average abundance and Apollinaris Mons is fourth highest. Our remaining volcanic and sedimentary regions show very low averages in K and Th, which is consistent with prior findings for the chemistry of Noachian volcanics [9]. The overall dispersion of K and Th values differs greatly between SCR and Isidis, despite their similar average values. In fact, Isidis' dispersion of K and Th values spans almost the entire range of measured K and Th abundances. Overall, there isn't much deviation from the linear trend fitted to the data from the majority of our analyzed regions, excluding Hellas and Eridania.

For our geophysical modelling results, we show the best-fit admittance model in Fig. 3A, which has a root-mean-square (RMS) of the misfit between the theoretical model and measured admittance of 1.34 mGal/km for the degree range 77-120. The error bounds on the admittance shown in Fig. 3A are computed from the relationship between admittance variance and correlation

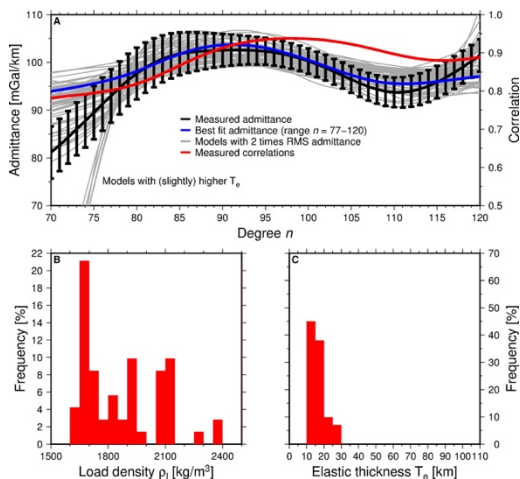


**Figure 3:** Localized admittance and correlation for the Arabia Terra area (centered on  $-5^{\circ}\text{E}, 25^{\circ}\text{N}$ , for a spherical cap with a radius of  $15^{\circ}$ ), including the best-fit theoretical admittance and models within two times this best fit (A). Histograms of the values for load density (B) and elastic thickness (C) for these models are also included.

[6]. Using the parameters from the collection of models that fit the admittance within two times the best-fit RMS, we investigate the spread in the parameter values to establish which parameters can be constrained. We find that the parameters that are best-constrained are the load density and elastic thickness. The overall density of SCR is consistent with pyroclastic-rich material [9] compared to that of unaltered Martian basalt [10]. The elastic thickness appears well-constrained, and the resulting values are low.

**Discussion:** K and Th abundances within SCR, are broadly inconsistent with aqueous alteration. If SCR functioned as a floodplain [11], or was subject to ubiquitous fluvial activity within the Noachian [12], then Th would become increasingly fractionated from K, resulting in a high K/Th ratio and a low Th abundance [7], which isn't observed. SCR also shows similar K and Th values to that of Isidis, whose impact-formed history resulted in km-scale thick olivine layers, that have remained relatively unaltered through time [13,14]. These olivine layers likely formed as a result of the initial impact, but subsequent, post-impact magmatism likely contributed to the wide range of K and Th values observed for Isidis [14]. Therefore, we interpret the similarity in K and Th values between Isidis and SCR as indicative of igneous processes, and as evidence against a narrative of aqueous activity emplacing a unique chemistry within SCR.

If volcanic eruptions of fine-grained material are responsible for the unique chemical signature we observe within SCR, then we expect the overall density of the area to be lower than that of volcanoes which erupt effusively. We observe a load density within the range of 1700-1900  $\text{kg/m}^3$ , which is consistent with pyroclastic material on Mars [15]. Furthermore, this density is similar to that of the MFF, which has been interpreted to have been emplaced through pyroclastic eruptions. Since we observe a strong correlation between the topography within SCR and a low elastic thickness value, we can also comment on a higher thermal state contributing to supervolcanic eruptions in Arabia. These results, coupled with our geochemical observations, support a narrative that diverges from a history of aqueous alteration. Instead, this narrative supports a sequence of supervolcanic eruptions, capable of resurfacing much of northwestern Arabia, which postdate the period of fluvial activity in the region.

**References:** [1] Michalski, J. R., & Bleacher, J. E. (2013). <https://doi.org/10.1038/nature12482> [2] Bandfield, J. L., Edwards, C. S., Montgomery, D. R., & Brand, B. D. (2013). <https://doi.org/10.1016/j.icarus.2012.10.023> [3] Bates, Augustus, et al (2018). <https://www.hou.usra.edu/meetings/lpsc2018/pdf/3010.pdf> [4] Hood, D. R., Judice, T., Karunatilake, S., Rogers, D., Dohm, J., & Skok, J. R. (2016). <https://doi.org/10.1002/2016JE005046> [5] Tanaka, K.L., Skinner, J.A., Jr., Dohm, J.M., Irwin, R.P., III, Kolb, E.J., Fortezzo, C.M., Platz, T., Michael, G.G., and Hare, T.M., 2014. <https://pubs.usgs.gov/sim/3292> [6] Grott M. & Wieczorek, M. A. (2012). <https://doi.org/10.1016/j.icarus.2012.07.008> [7] Taylor, G. J., Stopar, J. D., Boynton, W. V., Karunatilake, S., Keller, J. M., Brückner, J., ... Hahn, B. C. (2006). <https://doi.org/10.1029/2006JE002676> [8] Goossens S. et al. (2017). <https://doi.org/10.1002/2017GL074172> [9] Ojha, L., Lewis, K., Karunatilake, S., & Schmidt, M. (2018). <https://doi.org/10.1038/s41467-018-05291-5> [10] Baratoux, D., Toplis, M. J., Monnerneau, M., & Gasnault, O. (2011). <https://doi.org/10.1038/nature09903> [11] Tanaka, K. L. (2000). <https://doi.org/10.1006/icar.1999.6297> [12] Goudge, T. A., Fassett, C. L., Head, J. W., Mustard, J. F., & Aureli, K. L. (2016). <https://doi.org/10.1130/G37734.1> [13] Hamilton, V. E., Christensen, P. R., McSween, H. Y., & Bandfield, J. L. (2003). <https://doi.org/10.1111/j.1945-5100.2003.tb00284.x> [14] Mustard, J. F., Ehlmann, B. L., Murchie, S. L., Poulet, F., Mangold, N., Head, J. W., ... Roach, L. H. (2009). <https://doi.org/10.1029/2009JE003349> [15] Ojha, L., & Lewis, K. (2018). <https://doi.org/10.1029/2018JE005565>